The Oxidation of Ferrocene in Sessile Toluene Macro- and Microdroplets: An Opto-Electrochemical Study

Joshua Reyes-Morales[a], Matthew W. Glasscott[a], Andrew D. Pendergast[a], Sondrica Goines[a], and Jeffrey E. Dick[a,b]*

*Corresponding author: jedick@email.unc.edu

[a]Department of Chemistry, The University of North Carolina at Chapel Hill, Chapel Hill, NC 27599, USA

[b]Lineberger Comprehensive Cancer Center, School of Medicine, The University of North Carolina at Chapel Hill, Chapel Hill, NC 27599, USA

Abstract: Obtaining mechanistic insight into interfacial electron and ion transfer processes remains imperative to developing a comprehensive understanding of synthetic and biological processes. There is fundamental interest in the coupled electron-ion transfer processes characteristic of heterogeneous reactions at three-phase boundaries comprised of two immiscible liquids and a solid electrode surface. To probe reactivity at the three-phase boundary, we report a multifaceted analysis of ferrocene (Fc) oxidation in toluene droplets of diverse sizes. In one experiment, we study Fc oxidation in a large toluene microdroplet. In a second experiment, we study Fc oxidation in an array of toluene nanodroplets. We performed each experiment with and without an ionic liquid, trihexyltetradecylphosphonium bis(trifluoromethylsulfonyl)amide. Upon Fc oxidation in the oil phase without supporting electrolyte, the Fc^+ cation, which is soluble in water, is expelled from the oil phase to maintain charge neutrality. Because Fc is only slightly soluble in water (~40 μM), reversing the scan to reduce Fc^+ in the aqueous phase generates a Fc precipitate adjacent to the three-phase boundary. This observation was confirmed by correlated optical microscopy. Increasing the voltammetric scan rate elucidated sequential versus concerted ion transfer mechanisms, which are shown to be highly dependent on the droplet size and the presence of trihexyltetradecylphosphonium bis(trifluoromethylsulfonyl)amide in the toluene phase. Differences in voltammetric responses are supported by finite element simulations.

Keywords: Ion-Transfer, ITIES, Voltammetry

Table of Contents Graphic:

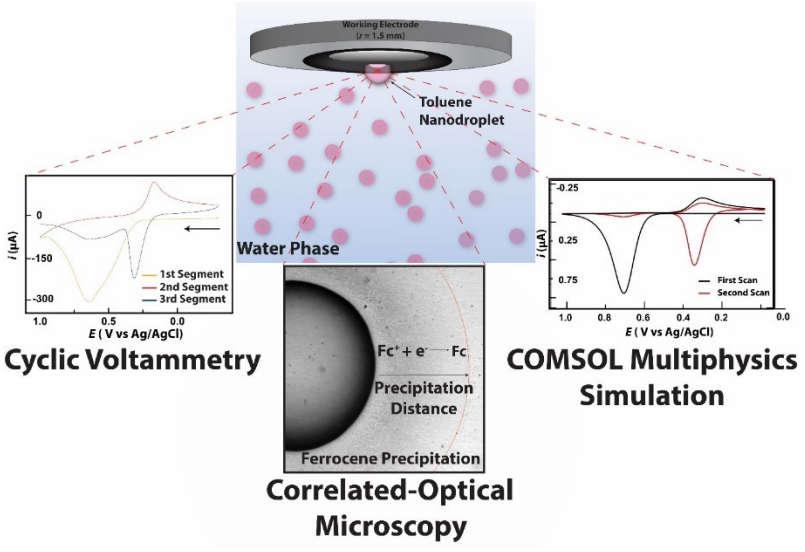

Introduction:

Transferring ions and electrons across physical boundaries in multi-phase systems plays a critical role in a multitude of industrial[1-4] and biological[5-7] processes. Electrochemistry is a powerful method to study interfacial charge transfer due to its sensitivity and intrinsic requirement of electron transfer across a metal|solution interface. More complex processes may be examined by incorporating an additional interface, such as an immiscible liquid, to form a three-phase system. Widely, reactions at the three-phase boundary have been of interest due to the applicability of multi-phase systems such as their use towards fuel cell design.[8]

Historically, the three-phase boundary (*i.e.*, the interface between two immiscible liquids and a solid surface) has been formed by placing a large liquid droplet on top of, but not entirely covering, an electrode surface. When this droplet-modified electrode is introduced into a liquid continuous phase that is immiscible with the droplet phase, voltammetric experiments on the three-phase boundary may be directly performed. Importantly, redox reactions which occur within the droplet phase require an ion-transfer step between the two liquid phases in order to maintain charge neutrality. This requirement may be exploited to isolate the reactivity of the three-phase boundary.[9] For instance, Schotz and co-workers hypothesized that removing the supporting electrolyte from the droplet phase promoted confinement of the redox reaction to the three-phase boundary due to a concerted electron-ion transfer process. This allowed them to study the electron transfer properties of Fc/Fc^+ within immobilized nitrobenzene droplets to probe reactivity at the three-phase boundary. [10] Marken and co-workers and Compton and co-workers pioneered the study of electroactive droplets/droplet arrays on electrode surfaces, determining that a lack of supporting electrolyte results in the absence of an appreciable double layer across the droplet|electrode interface.[11-17] Aoki and co-workers studied the oxidation of ferrocene (Fc), a well-behaved one-electron redox molecule, in microliter oil droplets immobilized on an electrode surface.[9, 18] Most recently, White and co-workers studied the electron-coupled phase transfer reaction of Fc by placing a platinum/iridium wire at the interface of 1,2-dichloroethane and water, correlating their results with COMSOL Multiphysics simulations.[19] Similarly, Stojek described a voltammetric study of Fc at a water/nitrobenzene interface with a microcylinder.[20]

Notably, in most of the previous cases, the authors studied electron and ion transfer properties by dissolving Fc in the oil phase (*e.g.*, dichloroethane, nitrobenzene), where it displays high solubility, and used water as the continuous phase. Fc is useful in that it may be readily oxidized to the hydrophilic Fc^+ cation, which may in turn be expelled from the oil phase to facilitate the ion transfer process. The literature suggests two possible mechanisms to describe Fc oxidation in a three-phase system.[9] A concerted mechanism, where the oxidation of Fc is coincident with the expulsion of the generated Fc^+ cation into the aqueous phase at the three-phase boundary, may be described as:

$$Fc_{oil} \rightarrow Fc^+_{oil} + e^- \textit{ (electron transfer)}$$

$$Fc^+_{oil} \rightarrow Fc^+_{aq} \textit{ (ion transfer)}$$

A sequential mechanism, where the oxidation of Fc is followed by the expulsion of a cation or the insertion of an anion originating from the supporting electrolyte, may be described as:

$$Fc_{oil} \rightarrow Fc^+_{oil} + e^- \textit{ (electron transfer)}$$

$$A^+_{oil} \rightarrow A^+_{aq} \textit{ (ion transfer)}$$

Or

$$B^-_{aq} \rightarrow B^-_{oil} \textit{ (ion transfer)}$$

Where *A* and *B* are cationic and anionic supporting electrolyte species, respectively.

To obtain mechanistic information regarding concerted *vs* sequential ion transfer mechanisms, the system of interest should meet certain requirements: 1.) The molecule undergoing the reaction must be soluble in only one phase so as not to transfer appreciably. 2.) The product of the molecule undergoing the reaction should be soluble in both phases, such that it may contribute to the charge balance mechanism. This is especially important if the intent is to study concerted transfer mechanisms. 3.) Any supporting electrolyte employed must be soluble in only one phase unless one is interested in how the transfer of electrolyte to maintain electroneutrality influences the voltammetric response. 4.) The reaction of interest must be driven within the potential window of the two phases.

Given the aforementioned requirements, the oxidation of Fc in the oil phase is a popular reaction to study. However, in previous voltammetric studies examining the concerted mechanism characterized by expulsion of the Fc^+ cation, there has been little consideration of Fc precipitation. White and co-workers noted that the peak currents of Fc^+ reduction and Fc oxidation in the aqueous

phase did not scale linearly with the square root of scan rate, indicating the redox process is not entirely diffusion controlled.[21] This precipitation is interesting because it highlights the importance of local surface concentrations that must be considered in the voltammetric analysis in such multiphase systems.

We report a set of experiments investigating the formation of ferrocene precipitates resulting from a voltammetric interrogation of the three-phase boundary formed by water, toluene, and an electrode surface. We studied both single, large microdroplets and arrays of nanodroplets. A schematic of the experiment is shown in **Scheme 1**. Fc is oxidized in the toluene droplet phase at 0.6 V vs. Ag/AgCl (yellow curve). In the reverse sweep, Fc^+ is reduced at a more negative potential (0.2 V vs. Ag/AgCl, red curve), representing the reduction of Fc^+ in the aqueous phase. Upon cycling in the positive direction, a large oxidation peak can be observed that was absent in the first scan, indicating the oxidation of Fc in the aqueous phase. We show that the observed current represents a concentration of Fc that is not soluble in water, consistent with previous work reporting a maximum aqueous solubility of Fc at 40 μM.[22] We further demonstrate through correlated optical microscopy experiments that a precipitate forms during the reduction of Fc^+ in the aqueous phase that may be stripped off at sufficiently positive potentials. The distance of the precipitate from the droplet oil phase agrees with what one would expect for freely diffusing Fc^+ in water.

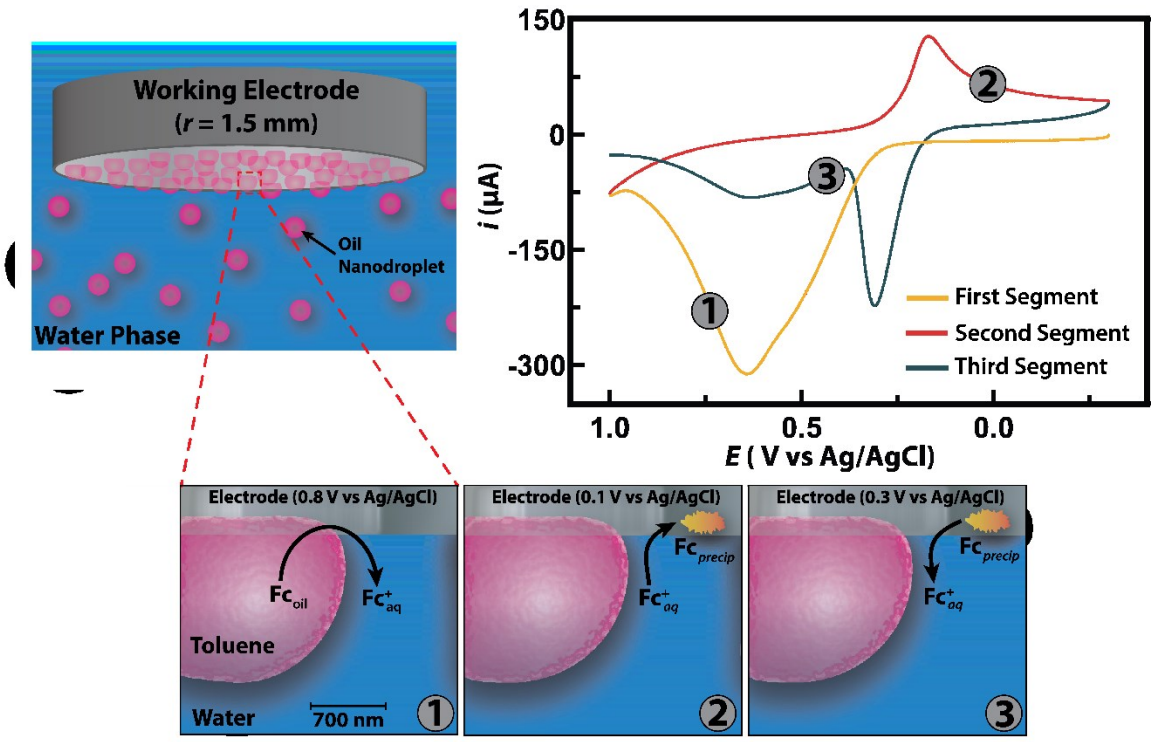

Scheme 1. Schematic representation of the experimental method to probe the formation of Fc precipitates in water. A glassy carbon working electrode was placed in an emulsion solution containing toluene microdroplets loaded with 50 mM Fc, which adsorbed to the surface for 5 minutes. By placing the electrode in a fresh solution of 250 mM KCl and sweeping the potential toward 1 V vs. Ag/AgCl at a scan rate of 1 V/s, the oxidation of Fc_{oil} to Fc^{+}_{oil} could be observed. Because of the lipophobicity of the Cl^{-} anion and the lack of supporting electrolyte in the toluene phase, the expulsion of the Fc^{+}_{oil} cation into the aqueous phase facilitated charge balance **(1)**. Reversing the sweep reveals a diffusion-limited reduction peak correlated with the reduction of Fc^{+}_{aq}, which formed a precipitate based on the limited solubility of Fc in water **(2)**. Sweeping the potential back toward 1 V vs. Ag/AgCl causes the Fc_{aq} precipitate to be stripped from the electrode surface **(3)**.

To probe the effect of supporting electrolyte, we introduced trihexyltetradecylphosphonium bis(trifluoromethylsulfonyl)amide (IL-PA) into the toluene phase and potassium chloride into the aqueous phase, where each electrolyte was specifically selected due to its insolubility in the opposite phase. Additionally, the use of IL-PA in the organic phase allowed us to consider how the viscosity of the solution may affect the ion-transfer mechanism across the toluene|water interface. To probe the effect of droplet size, we performed cyclic voltammetry using a large, sessile droplet (r = 150 μm) and an array of microdroplets (r = 894 nm) with and without IL-PA. We made two interesting observations from these experiments. The first observation is that both droplet sizes lacking IL-PA present similar voltammetric behavior characterized by the expulsion of Fc^{+} into the aqueous phase after the oxidation of Fc (concerted electron-ion transfer). The second observation is that having IL-PA present appears to alter the

mechanism. In the sessile droplet experiment, reversible behavior within the droplet phase can be observed (*i.e.*, the classical diffusion limited oxidation of Fc in a single phase). Similar to the experiments lacking IL-PA, the microdroplet array experiments exhibit no such reversibility, suggesting that the Fc^+ cation is being expelled from the toluene phase. We attribute this specific finding to the rapid rate of mass transfer and enhanced relative three-phase-boundary-surface-area to droplet-volume ratio, permitting a larger fraction of the electrogenerated Fc^+ to participate in a concerted electron-ion transfer mechanism. This finding was cross-examined and supported semi-quantitatively using COMSOL Multiphysics simulations. Collectively, we demonstrate that coupling optical microscopy, cyclic voltammetry, and finite-element simulations provides deeper insights into interfacial charge transfer reactions and possible coincident precipitation reactions.

Materials and Methods:

2.1 Reagents and Materials

1,2-dichloroethane (DCE, 99.8%), Toluene (99.8%), Ferrocene (98%), Ferrocenium hexafluorophosphate (97%) and Trihexyltetradecylphosphonium bis(trifluoromethylsulfonyl)-amide (IL-PA, ≥95.0%) were obtained from Sigma-Aldrich and used without further purification. Potassium Chloride (99.9%) was purchased from Fisher Scientific. Potassium chloride was dissolved in nano-pure water (18.2 MΩ·cm). The glassy carbon macroelectrode (3 mm diameter) and the Ag/AgCl reference electrode (stored in a 1 M KCl solution) were purchased from CH Instruments (Austin, TX). Between experiments working electrodes were polished, using 1 μm and 0.3 μm alpha alumina powder (CH Instruments), and sonicated to remove excess alumina.

2.2. Instrumentation

The emulsion solutions were prepared using a Q500 ultrasonic processor (Qsonica, Newtown, CT) with a microtip probe. Dynamic Light Scattering (DLS) was used to obtain the average size of the droplets where the data is available in the supporting information file from **Figure S2** to **Figure S4**. The equipment used for the DLS was a Zetasizer Nano ZS (Malvern, Westborough, MA). The electrochemical characterization was performed using cyclic voltammetry. The instrument used for these measurements was a CHI model 601D potentiostat (CH Instruments, Austin, TX). The reference electrode was a Ag/AgCl stored in a solution of 1 M KCl. The reference electrode was calibrated with a well-known redox couple of

ferrocene/ferrocenium (**Figure S1**). A glassy carbon rod was used as a counter electrode for most of the experiments, except for the correlated-optical microscopy experiments.

2.3 Preparation of solutions

Milli-Q water (18.2 MΩ·cm) was used to prepare all aqueous solutions. For voltammograms in **Figure 1** examining the aqueous electrochemistry of Fc^+, 0.5 mM Fc^+ hexafluorophosphate was prepared in 10 mL of an aqueous solution of 250 mM KCl. When adding Fc^+ hexafluorophosphate to the water, the solution developed a deep green color and small precipitates formed; thus, the solution was sonicated for 20 minutes.

The solution for the correlated optical-microscopy experiment presented in **Figure 2** and **Figure 3** was prepared by adding 0.1 µL of the toluene phase containing 50 mM Fc both with and without 40 % IL-PA in a dish. The glassy carbon macroelectrode was placed where the droplet adsorbed to the surface. A solution of water containing 250 mM KCl was added to the dish for a total volume of 2 mL. The solution was not sonicated.

To prepare the oil-in-water emulsions for the experiments which results are presented in **Figure 4**, 100 µL of toluene with 50 mM Fc with or without 40 % v/v IL-PA was placed in a Wheaton Science Products Glass 20 mL Scintillation Vial. and added to 10 mL of an aqueous solution of 250 mM KCl in water. Then the solution was sonicated with a Q500 ultrasonic processor. In the case of the sessile droplets, the solution was not sonicated because they were adsorbed to the electrode surface.

2.4 Correlated Microscopy

Correlated electrochemical and optical experiments were facilitated using a variable fluorescent bandpass hyperspectral imaging system composed of a Lambda LS xenon arc lamp (Sutter Instrument Company, Novato, CA), a Leica CTR advanced electronics box (Leica Microsystems, Germany), a Leica SP box LMT200 (Leica Microsystems, Germany), a Leica DMi8 inverted microscope (Leica Microsystems, Germany), a Leica DFC7000 GT camera (Leica Microsystems, Germany), a Lambda SC SmartShutter controller (Sutter Instrument Company, Novato, CA), two Lambda VF-5 tunable filter changers (Sutter Instrument Company, Novato, CA), and a Lambda 10-3 optical filter changer and SmartShutter control system (Sutter Instrument Company, Novato, CA). The excitation tunable filter changers were tuned to 700 nm in order to

obtain the images.[23] For correlated electrochemical analysis, a stepper and piezo positioner/controller (CH Instruments, Inc., Auston, TX) was assembled on top of the microscope stage to hold the electrode in place during the measurements. The positioner/controller is mobilized by a 920D bipotentiostat (CH Instruments, Inc., Austin, TX). A 3 mm glassy carbon inlaid disk electrode were purchased from CH Instruments to be used as the working and reference electrodes, respectively. An Ag/AgCl (1 M KCl) reference electrode was purchased from CH instruments. Pt wire was used as the counter electrode. The electrode was brought into focus at 10x or 20x, and cyclic voltammetry was conducted to capture the simultaneous optical and electrochemical signal resulting from the oxidation of Fc in the toluene droplet system.

Results and Discussion:

Many previous reports on the oxidation of Fc at the three-phase boundary do not seem to evaluate precipitation. Accordingly, we elected to directly evaluate the reduction of Fc^+ in water to eliminate the complexity introduced by the three-phase system. Fc^+ hexafluorophosphate (0.5 mM) was dissolved in water containing 250 mM KCl. The salt dissolution resulted in a deep green color, indicative of the presence of Fc^+ (**Figure S5**). Because various comments exist in the literature regarding the decomposition kinetics of Fc^+ ions in aqueous[24] and non-aqueous[25-26] electrolyte solutions, we prepared fresh solutions for each experiment and ensured the observed voltammetric peaks could be correlated to the redox behavior of the Fc/Fc^+ couple. Contrary to what one would expect for a freely diffusing species, a voltammogram of Fc^+ in water, given in **Figure 1**, presents a bell-shaped before the current returns to baseline. This shape is generally associated with surface-controlled processes. Thus, we hypothesized that the reduction of Fc^+ resulted in the precipitation of Fc on the electrode surface, which was stripped off on the reverse sweep to generate the observed oxidation peak. We note that the re-oxidation of the precipitate resembles an adsorbed layer and not necessarily the oxidation of a solid material on an electrode surface. One important experimental aspect to note that may complicate analysis is that the hydrophobic droplets are adsorbed onto the electrode surface, and there will be an interplay in terms of dissolution upon precipitate oxidation.

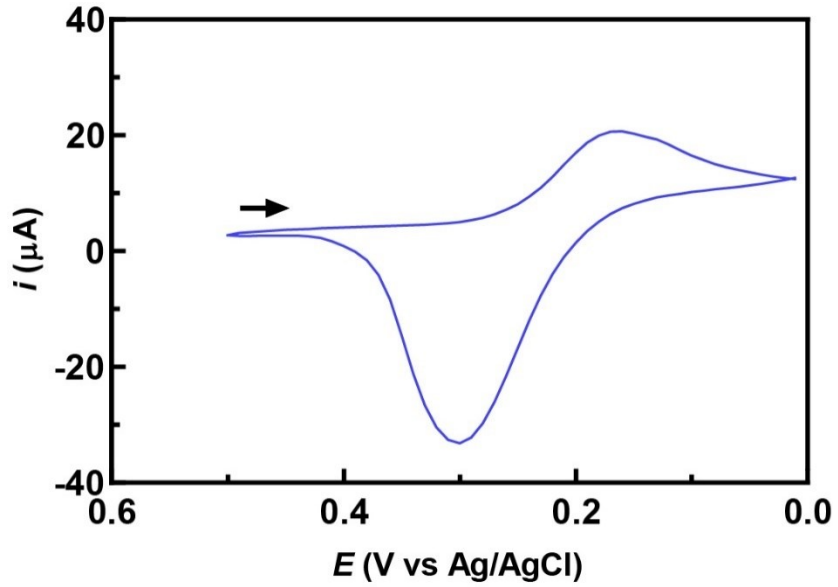

Figure 1 – Cyclic voltammogram of 0.5 mM Fc^+ hexafluorophosphate dissolved in water containing 250 mM KCl at 200 mV/s using a 3 mm diameter glassy carbon electrode. The voltammogram starts at 0.5 V vs. Ag/AgCl scanning toward the negative direction to first reduce Fc^+ to Fc.

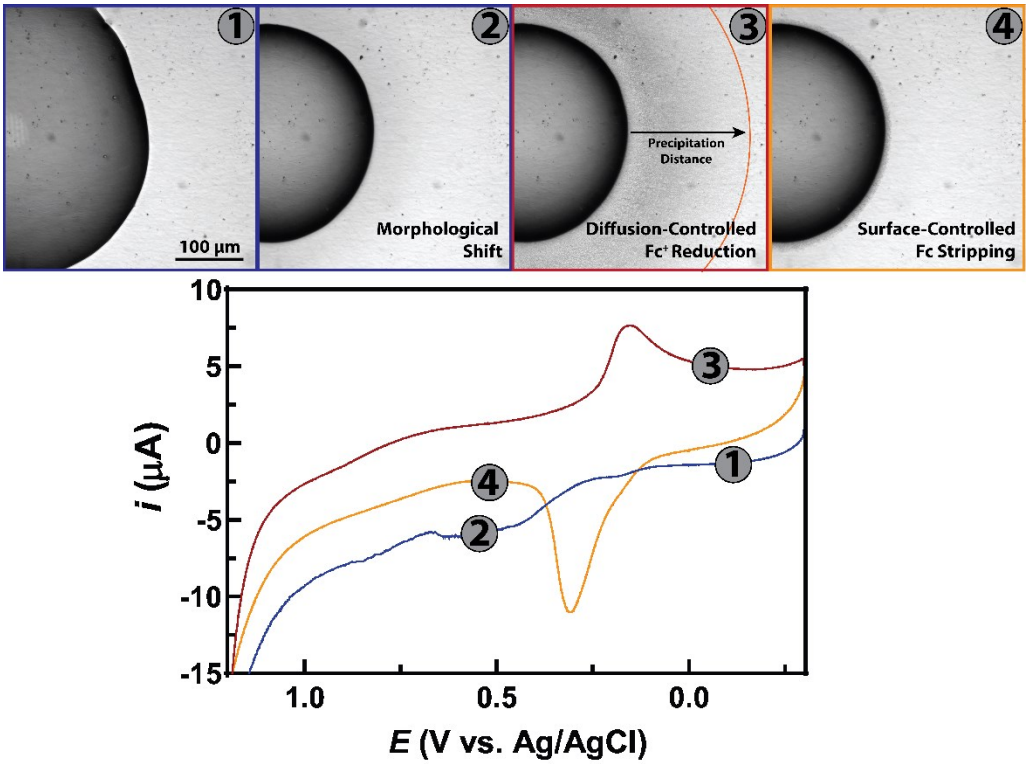

Figure 2 - Oxidation of 50 mM Fc within a toluene sessile droplet at 200 mV/s correlated with optical microscopy. The initial morphology of the droplet on the glassy carbon electrode **(1)** is observed to shift upon sweeping the potential toward 1 V vs. Ag/AgCl commensurate with the oxidation of Fc_{oil}, giving rise to irregularity in the anodic current **(2)**. The Fc^+_{oil} cation is expelled from the oil phase to maintain charge neutrality. The return sweep shows the

reduction of Fc^{+}_{aq} correlated with the appearance of a Fc_{aq} precipitate immediately about the droplet circumference extending for 190 μm **(3)**. The third CV segment indicates that the Fc_{aq} precipitate may be stripped off the surface **(4)**.

To optically probe this phenomenon, the electrochemical response was correlated with microscopy experiments (**Figure 2**). Here, a large droplet of toluene was loaded with 50 mM Fc and positioned on a glassy carbon surface, which was subsequently submerged in a solution of 250 mM KCl within the focal plane of the objective. Within **Figure 2**, Point 1 represents the beginning of the voltammetric scan, where the oxidation of Fc in water cannot be observed. At Point 2, Fc is oxidized in the toluene phase, and a slight shift in morphology of the droplet occurs at 0.6 V vs. Ag/AgCl (giving rise to instability in the voltammogram as the effective electrode area changes after ~0.2 V). This change in morphology can also be seen in the correlated optical image (optical image 1 *vs* optical image 2). During the oxidation of Fc in the toluene phase, Fc^{+} is expelled from the droplet to maintain electroneutrality. We note that the droplet initially changed in morphology, but no changes were observed as a function of potential after this initial change in morphology.

When the scan is reversed, the Fc^{+} in the aqueous phase is then reduced at Point 3. The optical image shows a drastic change in contrast around the droplet, which we interpret to be the precipitation of Fc onto the glassy carbon electrode. For a voltammetric sweep rate of 200 mV per second, Fc oxidation in toluene occurs at ~0.5 V, and Fc^{+} reduction in water at 0.3 V, the amount of time Fc^{+} has to diffuse from the droplet is *ca.* 8 seconds. Given $\delta = \sqrt{2Dt}$, where δ is the diffusion distance, D is the diffusion coefficient of Fc^{+} in water[21], and t is time, the distance Fc^{+} can diffuse is ~196 μm. This value is similar to the optically measured precipitation width of 190 μm. Discrepancies may be explained by the inability to resolve Fc precipitates furthest from the droplet interface and the approximated diffusion coefficient of Fc^{+} used for the calculations.

These observations indicate that when Fc^{+} is reduced at the electrode surface at concentrations exceeding the solubility limit of Fc, Fc precipitates. Upon cycling the potential to more positive values, the oxidation (anodic stripping) of the precipitated Fc can be observed with surface-bound, bell-shaped character (**Figure 2**, yellow curve). After this sweep, the contrast in the optical image outside the droplet returns to the initial state, and the oxidation of Fc in the toluene droplet is not appreciable on the subsequent scan. The lack of Fc oxidation in subsequent scans is indicative of the concerted electron-ion transfer mechanism, which expels each Fc^{+} cation

from the oil droplet as it is generated (*vide infra*). To validate the electrolysis time in the voltammetry shown in Figure 2, one can take advantage of bulk electrolysis theory to estimate the amount of time it takes to consume all ferrocene in the toluene droplet. The consumption of ferrocene can be modeled by:

$$i = i_o e^{-\frac{mAt}{V}} \text{ Eq 1}$$

Where i is the current, i_0 is the initial current ahead of electrolysis, m is the mass transfer coefficient of ferrocene, A is the electrode area, t is time, and V is the cell volume. Solving for time, we arrive at:

$$t = -\frac{V}{mA}\ln(\frac{i}{i_0}) \text{ Eq 2}$$

This equation allows us to calculate the time it takes to consume 99% (i/i_0 = .01) of ferrocene in the droplet. The mass transfer coefficient for ferrocene is 0.00002 m/s, and the area of the electrode with radius 150 μm is $7x10^{-8}$ m^2. The best estimate for the volume of the droplet from the optical photo is ~$7x10^{-12}$ m^3. Using these numbers, we arrive at a consumption time of several tens of seconds. The sweep rate in Figure 2 is 200 mV/s over the range of -0.25 to 1.2 V. This sweep range is 2.9 V, and the total amount of time it takes for the voltammetry to end is 14.5 seconds. Thus, the observed electrolysis times for the system is within the same order of magnitude as the above calculations.

In this study, we are interested in how the geometry of the droplet system may affect the observed voltammetry. In previous studies of three-phase electrochemistry, there is a question of where electrons and ions transfer. Compton and co-workers have handled this in a previous paper[17] observing the reduction of cuprate ions to copper metal and subsequently analyzing the electrodeposited copper with electron microscopy. These authors found that depending on relative concentrations of ions, the growth of copper will occur either at the three-phase boundary or inside the droplet.

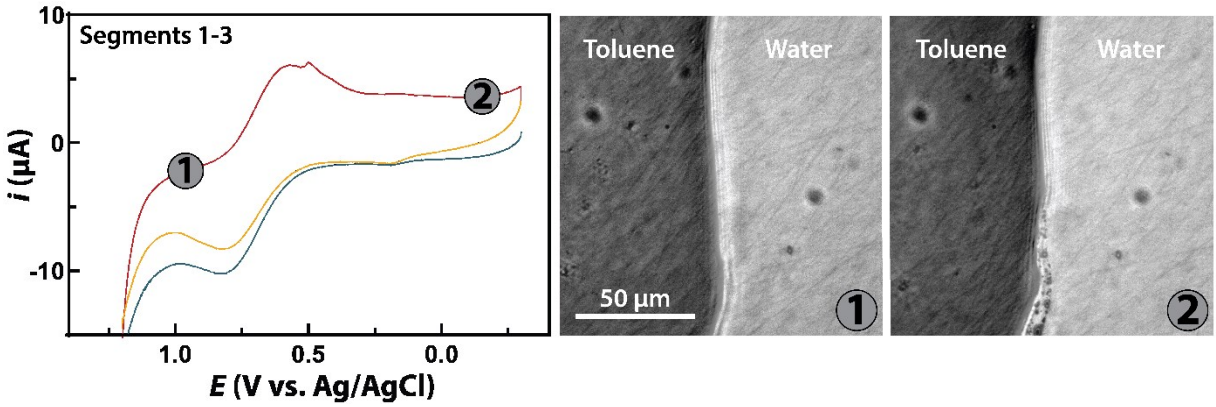

Figure 3 - Oxidation of 50 mM Fc within a 60/40 toluene/ionic liquid sessile droplet at 200 mV/s correlated with optical microscopy. The cyclic voltammogram was obtained using a glassy carbon electrode. Segment 1 shows the peak oxidation of Fc_{oil} at 0.8V vs. Ag/AgCl, while segment 2 reveals a reversible reduction of Fc^{+}_{oil} with the ionic liquid mediating charge balance **(1)**. Following the reduction peak at 0.6 V vs. Ag/AgCl, no precipitate is observed in the aqueous phase surrounding the droplet. A shift in the droplet morphology at the oil|water boundary **(*2*, bottom-center)** correlated with the reductive current spike at 0.5 V vs. Ag/AgCl observed in the voltammogram.

However, when IL-PA is introduced into the toluene droplet, minimal Fc^{+} is expelled into the aqueous phase upon Fc_{oil} oxidation. Shul et al. hypothesized that introducing IL-PA into the toluene phase facilitates the ion transfer of chloride into the oil phase to maintain electroneutrality.[23] Though the exact mechanism requires further evaluation, it appears the introduction of IL-PA permits ion transfer by a species other than Fc^{+}, representing a shift to a sequential electron-ion transfer mechanism. **Figure 3** exhibits a cathodic peak around 0.6 V vs. Ag/AgCl, indicating the reduction of Fc^{+} to Fc in the oil phase. This peak was only evident when IL-PA is present in the toluene phase. In the optical microscopy images in **Figure 3**, the dark contrast as presented in **Figure 2** is no longer visible, which further indicates that Fc^{+} is not expelled from the droplet in a concerted electron-ion transfer process. Interestingly, the spike located in the reduction wave correlated to a shift in the toluene/water interface, which can be observed in the lower half of optical image 2 (**Figure 2**). We note that shifts of this nature are permanent upon subsequent scans.

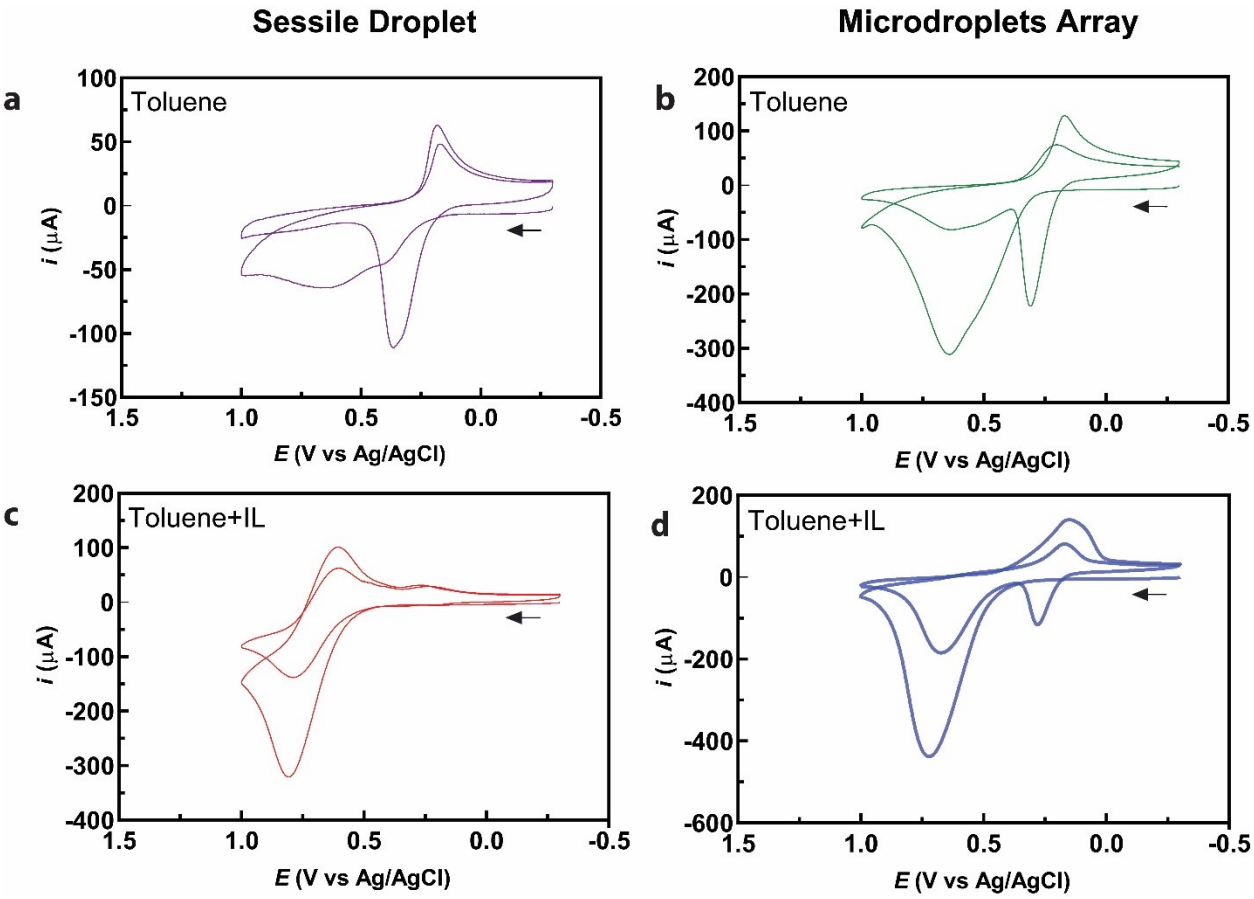

Figure 4 - Cyclic voltammograms of 50 mM Fc within either sessile droplets or microdroplets of toluene with and without 40 % v/v IL-PA at 1 V/s using a 3 mm diameter glassy carbon electrode. For the microdroplets, the radius with and without IL-PA was reported as 1141 nm and 894 nm, respectively. In panel **a** and **b**, the mechanism reflects Fc^+ expulsion following Fc oxidation in the oil phase. Fc^+ in the aqueous phase then undergoes reduction to a Fc precipitate, which may be stripped off when the scan is reversed. The addition of IL-PA in **c** and **d** reveals a cathodic peak corresponding to Fc^+ reduction in the sessile droplet, which is absent in the voltammogram of the microdroplet system.

While investigating Fc precipitates and the effect of ionic liquid on the electron-ion transfer mechanism, we observed an unexpected difference in the redox behavior of Fc in a large sessile droplet *vs* microdroplet arrays in the presence and absence of IL-PA. In **Figure 4a** and **4b**, the comparison of the redox behavior of Fc in a sessile droplet and microdroplets is depicted. As expected, the magnitude of the current for the microdroplet array system is larger than that of the single sessile droplet due to the perimeter amplification (*vide infra*). However, there is a clear difference in the redox behavior between the two systems containing IL-PA. From the voltammogram of the sessile droplet system containing IL-PA, the reversible reduction of Fc^+_{oil} to Fc_{oil} can be observed (**Figure 4c**), suggesting a sequential electron-ion transfer process. Conversely, the microdroplet system containing IL-PA seemingly exhibits a concerted electron-

ion transfer mechanism, as Fc^{+}_{aq} reduction and Fc_{aq} stripping is observed (**Figure 4d**). The difference may be explained by considering the mechanism of ion transfer, which depends on the spatial coordinates of the oxidation event. If Fc is proximal to the three-phase boundary upon oxidation, the Fc^{+} cation may be expelled to maintain charge balance.[11] However, if the oxidation occurs far from the boundary, the IL-PA or an impurity associated with the ionic liquid may facilitate the ion transfer process. Contrasting the geometry of sessile droplets and microdroplet arrays provides insight into the possibility of sequential *vs* concerted electron-ion transfer mechanisms. Namely, using arrays of microdroplets maximizes the perimeter (*i.e.*, three-phase boundary) compared to studying one relatively large sessile droplet. Here, the electrochemical signal at the phase boundary can be amplified by almost three orders of magnitude due to the collective perimeter of the droplets. For instance, a large microdroplet has a perimeter on the order of millimeters, whereas an array of a million droplets with radii of ~800 nm have a perimeter on the order of meters. It should be noted that the ferrocenium ion-transfer is not dependent on the concentration of ferrocene in the toluene droplet (**Figure S6**). Thus, we hypothesize Fc^{+} will be expelled rapidly from microdroplets due to the rapid mass transfer and an enhanced three-phase boundary area within microdroplets.[21]

To test this hypothesis, COMSOL Multiphysics V5.5 finite element simulations were prepared to model voltammetry of single toluene sessile droplets for semi-quantitative analysis. We note that the analysis is semi-quantitative given the complex nature of introducing precipitation into the COMSOL model, which adds adjustable parameters are not readily available in the literature or readily obtained experimentally. The electrochemical cell was modelled as a static toluene droplet adsorbed on a conductive electrode surface surrounded by an aqueous continuous phase. To approximate the observed Fc precipitation in the aqueous phase, a surface reaction condition boundary was imposed at the electrode surface in the aqueous phase to form an adsorbed Fc species with an equilibrium constant significantly favoring the adsorbed form. At the toluene|water boundary, phase transferring was imposed such that Fc^{+} transferred to the aqueous phase following Fc precipitation. Another condition stated was that no electrolyte was dissolved in the oil-droplet phase. Additional simulation details are provided in the **section V** of the **Supporting Information** file.

To relate droplet geometry and voltammetric mechanism, voltammetry was simulated at larger hemispherical sessile droplets.

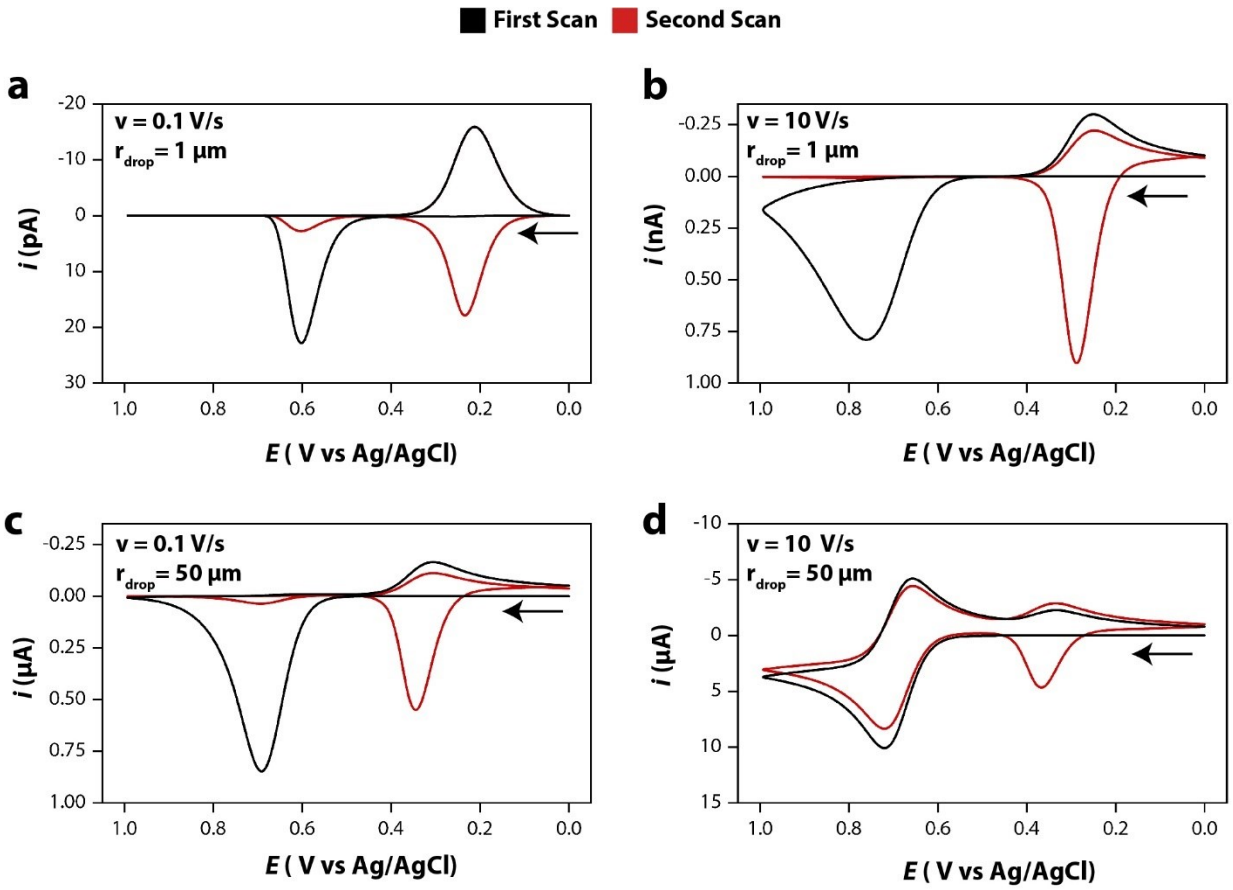

Figure 5- Simulated cyclic voltammograms of 1 µm radius microdroplets (a-b) and 50 µm radius sessile droplets (c-d) revealing multipeak behavior consistent with experimental voltammograms. All voltammograms were simulated over two full voltammetric sweeps with the black trace corresponding to the first sweep and the red trace corresponding to the second. For the simulated microdroplet voltammograms in panel **a** and **b**, no Fc^+ reduction peak was observed in the organic droplet phase, indicating complete transferring of the Fc^+ species into the aqueous bulk phase at both 0.1 and 10 V/s scan rates. For the 50 µm radius sessile droplet at a scan rate of 0.1 V/s, as presented in panel **c**, this voltammetric behavior is conserved. However, in panel **d**, a scan rate of 10 V/s does not provide sufficient time for Fc^+ inside the organic droplet to completely escape, resulting in the emergence of a new Fc^+ oxidation wave in the organic phase during both the first and second voltammetric cycles.

A simulated cyclic voltammogram of a 1 µm radius droplet at a scan rate of 0.1 V/s is presented in **Figure 5a** demonstrating two peaks behavior that can be attributed to the Fc oxidation in the toluene phase and both Fc oxidation and Fc^+ reduction in the aqueous phase. During the initial forward scan (black trace), Fc oxidation is observed in the toluene phase; however, upon reversing the scan at 1 V vs. Ag/AgCl, no associated Fc^+ reduction peak is observed until the formal potential of the Fc/Fc^+ couple in the aqueous phase is reached. On the second forward scan (red trace), Fc oxidation is observed in both the aqueous and organic phases while Fc^+ reduction is once again limited to the aqueous phase, consistent with experimental voltammetry (see **Figure 4b**). At a faster scan rate of 10 V/s, similar voltammetric behavior is observed in **Figure 5b**. More

specifically, one can observe the absence of Fc^+ reduction in the organic phase and the two peaks Fc oxidation on the second voltammetric scan, indicating complete transfer of generated Fc^+ from the toluene phase into the aqueous continuous phase. To explore the effects of geometry on mass transfer within the droplet system, voltammetry was additionally modelled at larger static hemispherical droplets with a radius of 50 μm. At a scan rate of 0.1 V/s, as presented in **Figure 5c**, the voltammetric behavior previously described is conserved, demonstrating sufficient time for Fc^+ generated in the droplet to diffuse to the toluene/water boundary and transfer into the bulk solution. However, at a faster scan rate of 10 V/s, a new Fc^+ reduction peak is observed in the organic droplet phase during both the first and second voltammetric sweeps, as presented in **Figure 5d**. For the larger droplet at a fast scan rate, some of the Fc^+ generated during the first forward scan in the organic droplet is capable of diffusing to the toluene/water boundary and transferring into the aqueous phase before a sufficient reducing potential can be reached on the reverse scan. As a result of these competing mass transfer and potential scan rate effects, the magnitude of the organic phase Fc^+ reduction peak is less than the associated organic phase Fc oxidation peak. Additionally, this Fc^+ transferring into the aqueous phase can be observed with the presence of a Fc^+ reduction wave in the aqueous phase during both voltammetric sweeps.

From these simulations, the mechanism of the experimental voltammograms can be explained in terms of intra-phase mass transfer, inter-phase redox mediator transferring, and surface equilibrium reactions to deconvolute multiphase complex voltammetric responses at the single droplet level. Due to the complex nature of the irreversible adsorption upon reduction of Fc^+ in the aqueous phase, we are unable to give a meaningful fit to the observed voltammograms. Again, we emphasize that the simulations validate our mass transfer hypothesis semi-quantitatively. A quantitative voltammetric fit would require insight into adjustable parameters, including adsorption constants. We also observed that the presence of IL-PA affects this mechanism, highlighting the importance of how the ionic liquid facilitates charge or influences the interfacial electric field that dictates charge transfer.

Conclusions:

Through correlated voltammetry and optical microscopy, we demonstrate mechanistic insight into the oxidation of Fc inside toluene droplets and subsequent ion transfer into the aqueous

continuous phase. Our results indicate that upon oxidation of Fc in the toluene phase, Fc^+ is expelled from the toluene phase to maintain electroneutrality. The voltammetric reduction of Fc^+ in water was also shown to be accompanied by the precipitation of Fc onto the electrode surface, which may be stripped off on a subsequent scan. The correlated opto-electrochemical methods presented here also elucidated irregular changes in the voltammetry that could be related to changes in droplet morphology on the electrode surface. Furthermore, we explain difference in voltammetric behavior for large droplets and droplets of micrometer dimensions in the presence and absence of IL-PA. In the absence of IL-PA, a similar mechanism was observed for a single sessile droplet and arrays of microdroplets, highlighting the importance of the interfacial electric field. In the presence of IL-PA, the rate of mass transfer and the boundary-area-to-volume ration is very high in microdroplets, increasing the probability of Fc^+ expulsion. Thus, the reduction of Fc^+ in toluene is not observed in the voltammetry, whereas it is observed in large sessile droplets. With the addition of COMSOL Multiphysics voltammetric simulations as a semi-quantitative analysis, we confirmed that rapid mass transfer in small droplets accounts for the difference in the observed voltammetry. Taken together, these experiments set a foundation for the study of complex reaction mechanisms at phase boundaries.

Supporting Information Available: This material is available free of charge *via* the Internet at *Journal of Electroanalytical Chemistry*.

AUTHOR INFORMATION

Corresponding Author

* jedick@email.unc.edu

Author Contributions

All authors have approved the final version of the manuscript.

ACKNOWLEDGMENT

This material is based upon work supported by the Chemical Measurement and Imaging Program in the National Science Foundation Division of Chemistry under Grant CHE-2003587

References:

(1) Hagfeldt, A.; Gratzel, M. Light-Induced Redox Reactions in Nanocrystalline Systems. *Chemical Reviews* **1995,** *95*, 49-68.

(2) Subramanian, V.; Wolf, E. E.; Kamat, P. V. Catalysis with Tio2/Gold Nanocomposites. Effect of Metal Particle Size on the Fermi Level Equilibration. *Journal of the American Chemical Society* **2004,** *126*, 4943-4950.

(3) Adams, D. M.; Brus, L.; Chidsey, C. E. D.; Creager, S.; Creutz, C.; Kagan, C. R.; Kamat, P. V.; Lieberman, M.; Lindsay, S.; Marcus, R. A.*, et al.* Charge Transfer on the Nanoscale: Current Status. *Journal of Physical Chemistry B* **2003,** *107*, 6668-6697.

(4) Eisenthal, K. B. Liquid Interfaces Probed by Second-Harmonic and Sum-Frequency Spectroscopy. *Chemical Reviews* **1996,** *96*, 1343-1360.

(5) Gray, H. B.; Winkler, J. R. Electron Tunneling through Proteins. *Quarterly Reviews of Biophysics* **2003,** *36*, 341-372.

(6) Langen, R.; Chang, I. J.; Germanas, J. P.; Richards, J. H.; Winkler, J. R.; Gray, H. B. Electron-Tunneling in Proteins - Coupling through a Beta-Strand. *Science* **1995,** *268*, 1733-1735.

(7) Kim, J. R.; Cheng, S.; Oh, S. E.; Logan, B. E. Power Generation Using Different Cation, Anion, and Ultrafiltration Membranes in Microbial Fuel Cells. *Environmental Science & Technology* **2007,** *41*, 1004-1009.

(8) Berg, P., Novruzi, A., & Volkov, O. (2008). Reaction Kinetics at the Triple-Phase Boundary in PEM Fuel Cells. *Journal of Fuel Cell Science and Technology, 5*(2). doi:10.1115/1.2821599

(9) Aoki, K.; Tasakorn, P.; Chen, J. Y. Electrode Reactions at Sub-Micron Oil Vertical Bar Water Vertical Bar Electrode Interfaces. *Journal of Electroanalytical Chemistry* **2003,** *542*, 51-60.

(10) Donten, M.; Stojek, Z.; Scholz, F. Electron transfer – Ion Insertion Electrochemistry at an Immobilised Droplet: Probing the Three-Phase Electrode-Reaction Zone With a Pt Disk Microelectrode. *Electrochemistry Communications* **2002**, 4, 324-329.

(11) Banks, C. E.; Davies, T. J.; Evans, R. G.; Hignett, G.; Wain, A. J.; Lawrence, N. S.; Wadhawan, J. D.; Marken, F.; Compton, R. G. Electrochemistry of Immobilised Redox Droplets: Concepts and Applications. *Physical Chemistry Chemical Physics* **2003,** *5*, 4053-4069.

(12) Marken, F.; Hayman, C. M.; Page, P. C. B. Phosphate and Arsenate Electro-Insertion Processes into a N,N,N ',N '-Tetraoctylphenylenediamine Redox Liquid. *Electrochemistry Communications* **2002,** *4*, 462-467.

(13) Qiu, F. L.; Ball, J. C.; Marken, F.; Compton, R. G.; Fisher, A. C. Voltammetry of Electroactive Oil Droplets. Part I: Numerical Modelling for Three Mechanistic Models Using the Dual Reciprocity Finite Element Method. *Electroanalysis* **2000,** *12*, 1012-1016.

(14) Ball, J. C.; Marken, F.; Qiu, F. L.; Wadhawan, J. D.; Blythe, A. N.; Schroder, U.; Compton, R. G.; Bull, S. D.; Davies, S. G. Voltammetry of Electroactive Oil Droplets. Part Ii: Comparison of Experimental and Simulation Data for Coupled Ion and Electron Insertion Processes and Evidence for Microscale Convection. *Electroanalysis* **2000,** *12*, 1017-1025.

(15) Laborda, E.; Molina, A.; Espin, V. F.; Martinez-Ortiz, F.; de la Torre, J. G.; Compton, R. G. Single Fusion Events at Polarized Liquid-Liquid Interfaces. *Angewandte Chemie-International Edition* **2017,** *56*, 782-785.

(16) Zhang, H. Z.; Sepunaru, L.; Sokolov, S. V.; Laborda, E.; Batchelor-McAuley, C.; Compton, R. G. Electrochemistry of Single Droplets of Inverse (Water-in-Oil) Emulsions. *Physical Chemistry Chemical Physics* **2017,** *19*, 15662-15666.

(17) Davies, T. J.; Wilkins, S. J.; Compton, R. G. The Electrochemistry of Redox Systems within Immobilised Water Droplets. *Journal of Electroanalytical Chemistry* **2006,** *586*, 260-275.

(18) Tasakorn, P.; Chen, J. Y.; Aoki, K. Voltammetry of a Single Oil Droplet on a Large Electrode. *Journal of Electroanalytical Chemistry* **2002,** *533*, 119-126.
(19) Weatherly, C. K. T.; Ren, H.; Edwards, M. A.; Wang, L.; White, H. S. Coupled Electron- and Phase-Transfer Reactions at a Three-Phase Interface. *Journal of the American Chemical Society* **2019,** *141*, 18091-18098.
(20) Bak, E.; Donten, M.; Stojek, Z. Three-Phase Electrochemistry with a Cylindrical Microelectrode. *Electrochemistry Communications* **2005,** *7*, 483-489.
(21) Faulkner, A. J. B. a. L. R., *Electrochemical Methods: Fundamentals and Applications*. 2 ed.; John Wiley & Sons: New York, New York, 2001.
(22) Wu, J. S.; Toda, K.; Tanaka, A.; Sanemasa, I. Association Constants of Ferrocene with Cyclodextrins in Aqueous Medium Determined by Solubility Measurements of Ferrocene. *Bulletin of the Chemical Society of Japan* **1998,** *71*, 1615-1618.
(23) Shul, G.; Adamiak, W.; Opallo, M. Ion Insertion into Ionic Liquid Supported Toluene Generated by Electrochemical Redox Reaction. *Electrochem. Commun.* **2008,** *10*, 1201-1204.
24) Huang, W. H., & Jwo, J. (1991). Kinetics of the Decomposition of Ferrocenium Ion and Its Derivatives. *Journal of the Chinese Chemical Society, 38*(4), 343-350. doi:10.1002/jccs.199100058
25) Hurvois, J., & Moinet, C. (2005). Reactivity of ferrocenium cations with molecular oxygen in polar organic solvents: Decomposition, redox reactions and stabilization. *Journal of Organometallic Chemistry, 690*(7), 1829-1839. doi:10.1016/j.jorganchem.2005.02.009
26) Singh, A., Chowdhury, D. R., & Paul, A. (2014). A kinetic study of ferrocenium cation decomposition utilizing an integrated electrochemical methodology composed of cyclic voltammetry and amperometry. *The Analyst, 139*(22), 5747-5754. doi:10.1039/c4an01325e.
(27) Glasscott, M. W.; Dick, J. E. Visualizing Phase Boundaries with Electrogenerated Chemiluminescence. *The Journal of Physical Chemistry Letters* **2020,** *11*, 4803-4808.
28) Scholz, F. (2016). *Electrochemistry of immobilized particles and droplets*. Springer International Publishing Switzerland 2015.